Green biosynthesis of silver nanocubes using the leaf extracts from *Eucalyptus macrocarpa*

Gérrard Eddy Jai Poinern[1,a], Peter Chapman[2], Monaliben Shah[1] and Derek Fawcett[1]

[1] Murdoch Applied Nanotechnology Research Group. Department of Physics, Energy Studies and Nanotechnology, School of Engineering and Energy, Murdoch University, Murdoch, Western Australia 6150, Australia
[2] Department of Chemistry, Curtin University of Technology, Bentley, Western Australia 6102, Australia
[a] Corresponding Author: g.poinern@murdoch.edu.au

Received 22 Mar 2013; revised 04 Apr 2013; accepted 04 Apr 2013; published 08 Apr 2013.

ABSTRACT: In this preliminary study, we present for the first time a facile and environmentally friendly process for the green synthesis of silver nanoparticles using the leaf extract from an indigenous Australia plant *Eucalyptus macrocarpa*. The synthesis process is performed at room temperature and the leaf extract acts as both reducing agent and stabilising agent. The synthesis process is clean, non-toxic and straightforward and does not need complex processing equipment. The formation of the silver nanoparticles was confirmed by UV-visible spectroscopy, X-ray diffraction, transmission electron microscopy and field emission scanning electron microscopy.

KEYWORDS: silver nanoparticles, green synthesis, *Eucalyptus macrocarpa*

1. Introduction

Metallic nanoparticles prepared from metals, such as copper (Cu), gold (Au) and silver (Ag) have attracted considerable interest in many fields such as medicine, biotechnology, materials science, photonics and electronics [1-4]. The size, shape and surface morphology of the nanoparticles can have a profound influence on its chemical, physical, optical and electronic properties [5, 6]. This is indeed the case for medical preparations that use Ag nanoparticles as their active antimicrobial ingredient, since the antimicrobial effect of the nanoparticles is attributed to their size and high surface area to volume ratio, which enables them to closely interact with the bacterial cell membrane [7]. Recent antimicrobial studies have shown that membrane damage and toxicity can result from the bio-sorption and cellular uptake of nanoparticles by bacteria [8]. However, the processes behind nanoparticle inhibition of bacterial growth are not fully resolved, but some studies have suggested that the size, shape and surface modifications could influence the antibacterial properties of the nanoparticles [8, 9]. Conventional methods of producing nanomaterials involve the use of expensive chemical and physical processes that often use toxic materials with potential hazards such as environmental toxicity, cytotoxicity and carcinogenicity [10]. Furthermore, during these processes there is a potential for toxic chemical species to be absorbed onto the surface of the nanoparticles which ultimately leads to adverse effects occurring during their application. Therefore, it is imperative to develop alternative chemical synthesis processes that can produce metal nanoparticles without the problems of environmental toxicity, cytotoxicity and carcinogenicity. In recent years, the challenge has been to optimise the usage of environmentally friendly, naturally occurring extracts for the synthesis of metal nanoparticles.

An attractive alternative to the traditional manufacturing techniques used for the production of nanoparticles involves using a green, environmentally friendly technology based on biological systems such as plants [11, 12], bacteria [13, 14], fungus [15, 16] and similar organisms [17, 18]. Synthesising nano-particles via biological systems offers a clean, nontoxic and environmentally friendly method with the potential to deliver a wide variety of nanoparticle types, sizes, shapes and morphologies. To be an effective alternative, the green biosynthesis process needs to address three important parameters, namely: 1) an environmentally friendly solvent medium; 2) an effective and benign reducing agent; and 3) a nontoxic capping agent to stabilize the particles and prevent particle agglomeration [4]. Out of the several biological systems mentioned above, the biosynthesis of nanoparticles at ambient temperature via leaf extracts from plants is a relatively straight-forward technique. A leaf extract is an abundant source of phytochemicals that can potentially function as both reducing agent and stabilizing agent for the synthesis of nanoparticles [19]. The use of leaf extracts also has the advantage of not needing any special culture preparation or isolation techniques that are normally required for bacteria and fungi.

For centuries, silver and silver compounds have been successfully used as an effective antimicrobial agent for the treatment of infections. Silver nanoparticles (Ag NPs), like its bulk counterpart have also been found to be an

efficient antimicrobial agent capable of interacting with the cell membrane, interfering and damaging cellular nucleic acids [20]. Recent studies have shown that Ag NPs possess both anti-bacterial and anti-inflammatory properties that can promote faster wound healing and as a result have been incorporated into wound dressings, pharmaceutical preparations and implant coatings [21-23]. Because of the biomedical importance of Ag NPs and the need for new environmental friendly processes, it is necessary to investigate plant flora for potential candidates that can act as both reducing agent and stabilising agent.

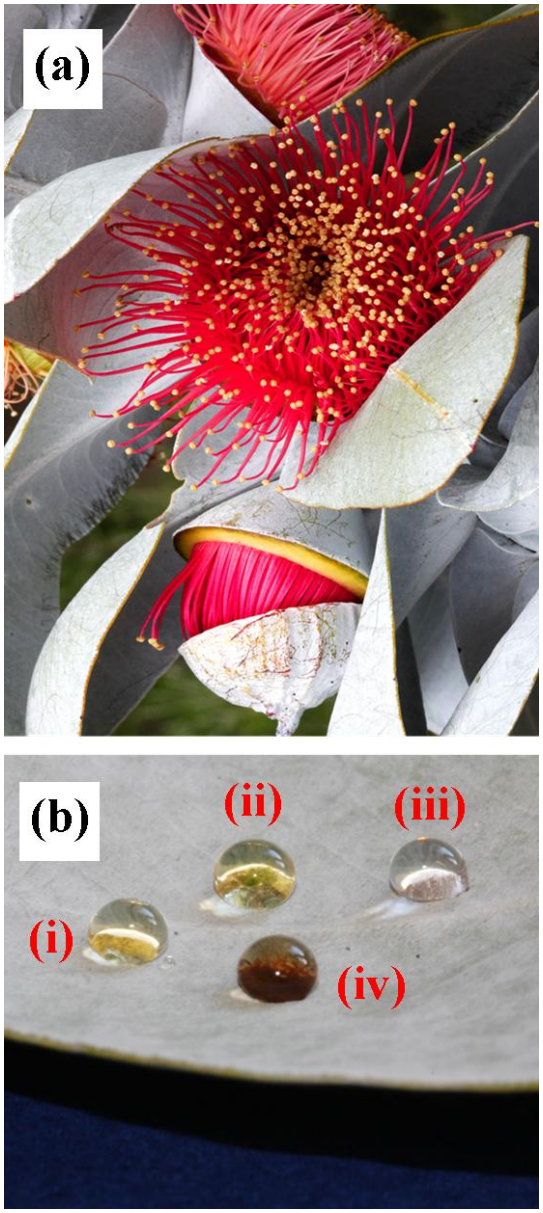

Figure 1. (a) *Eucalyptus macrocarpa* with its distinctive silvery foliage and prominent red flowers, (b) droplets consist of: (i) raw leaf extract; (ii) solution of Ag nanoparticles; (iii) pure $AgNO_3$ solution; and (iv), solution s_1 consisting of $AgNO_3$ and leaf extract solution (1:1).

The South West corner of the Australian continent is a global biodiversity hot spot and is also the indigenous region of the exquisite *Eucalyptus macrocarpa*, which is also known as the *Rose of the West or the Mottlecah* [24, 25]. The Mottlecah is easily recognized by its beautiful silvery foliage, which consists of distinctive ovate shaped leaves that can grow up to 12 cm in length and has prominent red flowers (see Fig. 1a). The silvery grey appearance of the plants leaves are the result of nano-structured features formed by the epicuticular waxes that give the leaves their remarkable wetting and self-cleaning properties which enhances the plants survival in its arid climate [26]. Because of its attractive floral arrangement, this particular eucalyptus is not an endangered species and has been successfully propagated across the west coast of Australia.

In this paper, we report for the first time the green synthesis of stable Ag NPs by the direct reduction of silver nitrate, ($AgNO_3$) via Mottlecah leaf extracts without using conventional stabilising agents. The advantages of using this approach include: 1) the leaf extract acts as both reducing agent and stabilising agent during the synthesis process; 2) the aqueous synthesis process is environmental friendly and produces no toxic waste products; and 3) the technique is simple, straight forward and does not require specialised equipment.

2. Materials and methods

2.1. Chemicals

The source of Ag^+ ions used throughout all nanoparticles synthesis procedures was silver nitrate [$AgNO_3$, (99.99%)] and was supplied by Sigma-Aldrich (Castle Hill, NSW, Australia). The Ag nanoparticles used as a control were synthesised by using sodium borohydride ($NaBH_4$) reduction of $AgNO_3$ in the presence of sodium citrate ($C_6H_5Na_3O_7$) as the stabilizing and capping agent. Both $NaBH_4$ and $C_6H_5Na_3O_7$ were purchased from Sigma-Aldrich (Castle Hill, NSW, Australia) and used without further purification. Milli-Q® water was used throughout all synthesis procedures involving aqueous solutions and was produced by a Barnstead Ultrapure Water System D11931 (Thermo Scientific Dubuque IA 18.3 MΩ cm^{-1}).

2.2. Leaf material and preparation of leaf extract

Eucalyptus macrocarpa or Mottlecah leaves were collected from several locations around the Murdoch University campus in Perth, Western Australia. A wide selection of healthy Mottlecah leaves, ranging from young to mature leaves was harvested from various locations on each plant. Generally, 5 locations were selected (top, north, south, east and west) and on average 10 leaves were taken from each of the locations. Both the adaxial and abaxial sides of the leaf were examined, with only healthy leaves free from damage being harvested. The leaves were washed several times with Milli-Q® water to

remove any dust or debris. After cleaning, 10 g of Mottlecah leaves were finely cut into small strips and then added to a 100 mL solution of Milli-Q® water. The aqueous mixture was then added into the blending bowl of an IKA® T25 Digital Ultra-Turrax® Homogenizer. The mixture was homogenized at 5000 rpm for 10 min at a room temperature of 24 °C. At the end of this time the solution was first filtered using a Hirsch funnel to remove leaf debris. This was followed by two further filtrations using a 0.22 µm Millex® (33 mm Dia.) syringe filter unit. At the end of the resulting filtration procedure, the leaf extract was placed in a glass vial ready for the synthesis of Ag nanoparticles.

2.3. Synthesis of Ag nanoparticles

The Ag nanoparticles used as the control were synthesised by first adding a 1.0 mL solution of 1 mM $AgNO_3$ to a 10 mL solution of Milli-Q® water while the solution was stirred vigorously. This was followed by adding a 1.0 mL solution of 1mM sodium citrate (stabilizing and capping agent) to the aqueous solution at room temperature (24 ˚C) and stirred for 10 minutes. The reduction of the Ag nanoparticles was initiated by the addition of a 1.0 mL solution of 0.01 M sodium borohydride to the aqueous solution. The reduction process was allowed to proceed at room temperature (24 ˚C).

Biological reduction of a 1.0 mL solution of 1 mM $AgNO_3$ was investigated using 3 solutions with varying amounts of leaf extract. The quantities of leaf extract used to make up the solutions consisted of 1 mL for s_1, 2 mL for s_2 and 3 mL for s_3. Once the $AgNO_3$ was added to each quantity of leaf extracts, the solutions were then vigorously stirred for 1 minute. The reduction process was allowed to proceed at room temperature (24 ˚C).

2.4. Leaf droplets

A clean Mottlecah leaf was selected, and laid flat in the horizontal plane to prevent the various droplet types from rolling off the leaf surface. Then using a fluid specific clean glass pipette fitted with a rubber bulb a series of 4 droplets were placed onto the leaf surface. The droplets consisting of: (i) raw leaf extract; (ii) solution of Ag nanoparticles; (iii) pure $AgNO_3$ solution; and (iv), solution s_1 consisting of $AgNO_3$ and leaf extract solution (1:1). The leaf and droplets were photographed over a period of time using a Canon EDS 600 D digital camera (Canon Inc, Tokyo Japan fitted with macro lens EF 100 mm 1:2:8 USM).

2.5. Characterisation of biologically reduced Ag NPs

All samples were examined and characterised using five advanced analysis techniques. These included: UV-visible spectrum analysis, X-ray diffraction spectroscopy (XRD), energy dispersive X-ray spectroscopy (EDAX), transmission electron microscopy and (TEM) field emission scanning electron microscopy (FESEM).

2.5.1. UV-visible spectrum analysis.

A series of samples were prepared. The first set consisted of three controls: 1) Milli-Q® water; 2) pure $AgNO_3$ solution; and 3) pre-filtered pure leaf extract (filtered twice, each time using a new Whatman 0.22µm syringe filter). The test solutions consisted of the 3 Ag colloids s_1, s_2 and s_3. The UV-visible spectra of each of the samples was then measured using a Varian Cary 50 series UV-Visible spectrophotometer version 3, over a spectral range from 200 to 1100 nm, with a 1 nm resolution over the first hr at room temperature of 24 °C.

2.5.2. XRD spectroscopy

After the end of each reduction procedure, samples for XRD examination were extracted from each glass vial using a clean glass pipette fitted with a rubber bulb. Then two to three drops of each sample were dispersed over the surface of a specific glass microscope slide. Then each glass slide was then dried under vacuum for a period of 4 hours. At the end of this time, the dried samples were then characterised using XRD spectroscopy. The XRD spectra were recorded at room temperature (22 °C), using a Bruker D8 series diffractometer [Cu K_α = 1.5406 Å radiation source] operating at 40 kV and 30 mA. The diffraction patterns were collected over a 2θ range from 15° to 80° with an incremental step size of 0.04° using flat plane geometry. The acquisition time was 2 seconds. The powder XRD spectrum was used to identify the size of the Ag particles and their crystalline structure. The particle size was calculated using the Debye-Scherrer equation [Equation 1] from the respective XRD patterns and estimated from both TEM and FESEM images.

2.5.3. EDAX spectroscopy

Each sample for EDAX examination was initially deposited onto a thin mica strip using a glass pipette, the mica strip was attached to a SEM stub using carbon tape. The samples were then dried under vacuum overnight. The following day, all samples were sputter coated with a 3 nm layer of Platinum. The samples were then examined using an Oxford Instruments EDS X-ray detector (EDAX) and Oxford Instruments energy dispersive X-ray detectors (EDS). The electron backscatter diffraction analysis (EBSD) used during the analysis was set with an EDS aperture of 60 µm and operated at 20kV.

2.5.4. TEM

The size and morphology of the Ag NPs was investigated using TEM. Sample preparation consisted of filtering the suspensions 2 times, each time using a new Whatman 0.22µm syringe filter. After filtration a single drop from each sample was deposited onto its respective carbon-coated copper TEM grid using a micropipette and then allowed to slowly dry over a 24 hour period. After sample preparation a bright field TEM study was carried out us-

ing a Phillips CM-100 electron microscope (Phillips Corporation Eindhoven, The Netherlands) operating at 80kV.

2.5.5. FESEM

Each sample for FESEM examination was initially deposited onto a thin mica strip using a glass pipette, the mica strip was attached to a SEM stub using carbon tape. The samples were then dried under vacuum overnight. The following day, all samples were sputter coated with a 3 nm layer of Platinum. The particle size and morphological features of the samples were investigated using a high resolution FESEM (Zeiss Neon 40EsB FIBSEM) at 5 kV with a 30 µm aperture operating under a pressure of 10^{-10} Torr.

3. Results and discussion

The present study reports the green synthesis of cubic Ag NPs by the biological reduction of aqueous silver ions using the leaf extract from Eucalyptus macrocarpa (Mottlecah). The water soluble ingredients present in the leaf extract were not only found to be a highly effective reducing agent, it also turned out to be an efficient stabilising agent. The formation of the Ag NPs could be easily monitored by the change in colour of the reactive mixture. The reactive mixture changes to a brown colour due to the excitation of surface plasmon vibrations of the formed Ag NPs. In the case of solution s_1 (1:1 ratio of $AgNO_3$ and leaf extract) the change in colour of the reaction mixture occurs within 10 minutes, see droplet (iv) in Fig. 1(b). There was no colour change in the control droplet, (iii), which only contains the pure aqueous $AgNO_3$ solution.

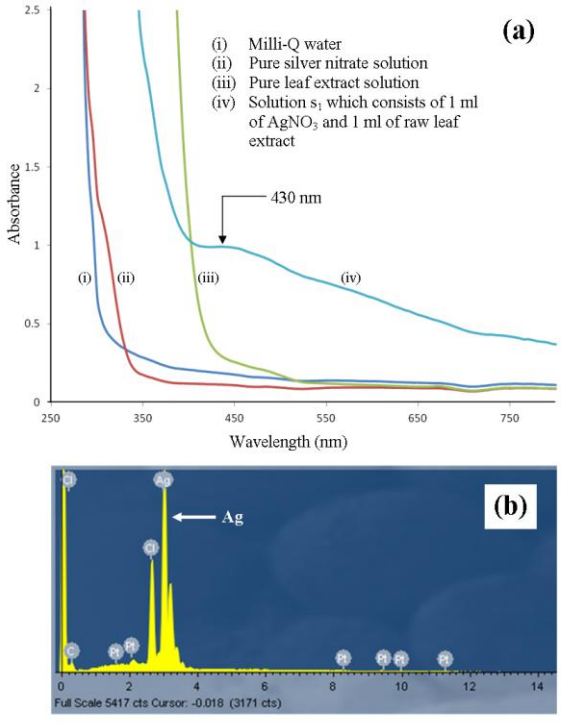

Figure 2. (a) UV-visible spectrophotometer analysis of Ag NPs synthesised using fresh *Eucalyptus macrocarpa* leaves, (b) EDAX spectra of synthesised Ag NPs

A qualitative evaluation of the reducing agents in the Mottlecah leaf extract could be made by comparing the colour change (mixture turning brown), the time of complete colour change and the concentration of $AgNO_3$ to leaf extract in the mixture. The reduction of the silver ions was quite rapid, with colloid s_1 (1:1) only taking 10 minutes to react. While in the case of colloid s_2 (1:2) it took 60 min to achieve the same colour change as s_1 and solution s_3 (1:3) took 90 minutes. This simple qualitative analysis reveals that the efficiency of the nanoparticle synthesis decreases with increasing amounts of leaf extract in the $AgNO_3$ to leaf extract colloid. The UV-Vis spectrum for solution s_1 (1:1) is presented in Fig. 2(a). The maximum absorbance occurs at 430 nm, which is similar to the maximum absorbance reported by Singh *et al* using ginger rhizome [27] and by Masurkar *et al* using *Cymbopogan citrates* (lemon grass) leaf extract [28]. The results of an EDAX spectroscopic examination of each colloid confirmed the presence of metallic Ag in each of the leaf extracts. A typical EDAX spectrum is presented in Fig. 2(b) for the s_1 solution and clearly indicates a significant metallic Ag peak.

To investigate the crystalline nature of the Ag NPs, dried Ag NP powder samples were investigated using XRD spectroscopy. The Ag crystalline phases present were found to be consistent with phases incorporated in the ICDD (International Centre for Diffraction Data) databases. The results of the XRD studies are presented in Fig. 3. Four diffraction patterns are presented for comparative purposes; the first is pattern (a), which represents the spectra of the leaf extract. Inspection of pattern (a) reveals that there are no diffraction peaks present. The second pattern (b) is the spectra of metallic Ag deposited on glass by Tollen's reaction, while pattern (c) is the spectra of Ag NPs synthesised via the reduction of $AgNO_3$ by sodium borohydride, with sodium citrate being used as the stabilizing and capping agent. Comparison of patterns (b), (c) and (d) reveals that the Bragg reflection peaks are present in all three. Examination of the dominant three peaks located at 38.5°, 44.5° and 64.5°, which corresponds to the (111), (200), and (220) lattice plane sets. The spectra of Ag NPs synthesised using the leaf extract, pattern (d) were then indexed to reveal a face centred cubic structure for the Ag powder sample. The crystalline size, $t_{(hkl)}$, of Ag NPs was calculated from the XRD pattern using the Debye-Scherrer equation presented in eq. (1) below:

$$t_{(hkl)} = \frac{0.9\lambda}{B\cos\theta_{(hkl)}} \quad (1)$$

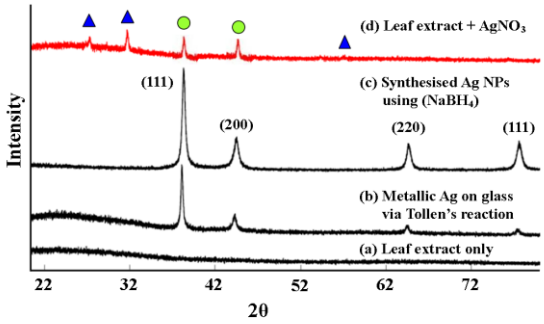

Figure 3. XRD patterns of leaf extracts and synthesised Ag NPs.The filled circles indicate peaks produced by mettallic Ag in the leaf extract treated with $AgNO_3$, while the filled triangles indicate new peaks being formed by the interaction between leaf extract and $AgNO_3$.

where, λ is the wavelength of the monochromatic X-ray beam, *B* is the Full Width at Half Maximum (FWHM) of the peak at the maximum intensity, $\theta_{(hkl)}$ is the peak diffraction angle that satisfies Bragg's law for the (h k l) plane and $t_{(hkl)}$ is the crystallite size. An estimate of the mean crystallite size using the FWHM of the (111) was calculated to be 38 ± 2 nm for the Ag NPs synthesised using the leaf extract.

The final XRD pattern in Fig. 3 is (d), which also reveals the presence of a number of other peaks in the leaf extract being treated with $AgNO_3$. The presence of metallic Ag in the leaf extract/ $AgNO_3$ mixture is indicated by the two diffraction peaks at 38.8˚ and 44.5˚, which correspond to the (111) and (200) lattice planes respectively. These peaks are indentified by filled circles in pattern (d). Inspection of pattern (d) also indicates the presence of two significant, but unidentifiable peaks and one extremely weak unidentifiable peak. All three peaks are indicated in pattern (d) by the presence of a filled triangle over the peak. Similar unidentifiable peaks resulting from the interaction between $AgNO_3$ and a fungus (*Aspergillus flavus*) have also been reported by Vigneshwaran *et al* [29]. The three unidentified peaks formed by the interaction between leaf extract and $AgNO_3$ are currently being investigated by the authors.

Figure 4(a) presents a typical TEM image of Ag NPs taken within 1 h after the reduction process. The image reveals spherical and non-spherical morphology, with a number of nanometre sized cubes clearly present these are circled in blue for easier identification. The spherical Ag NPs range in size from 10 to 100 nm, while the nanometre sized cubes range in size from 10 to 50 nm. At this point in time there are also a few nanometre size triangles present. Figure 4(b) presents an FESEM image of Ag nanocubes taken 90 minutes after the initial reduction process, at this point in time the cubes range from 50 to 200 nm. If the colloidal solution is allowed to age for several hours, many of the Ag NPs grow into micrometre size particles, which are predominantly cubic in structure as shown in Fig. 4(c). The typical side dimension of the larger micrometre scale Ag cubes was found to be around 1 µm. There are also many nanometre structures still present along with the organic matrix of the leaf extract. At this stage there are relatively few spherical NPs, but there are small numbers of triangular structures, these are circled in red for easier identification in Fig. 4(c).

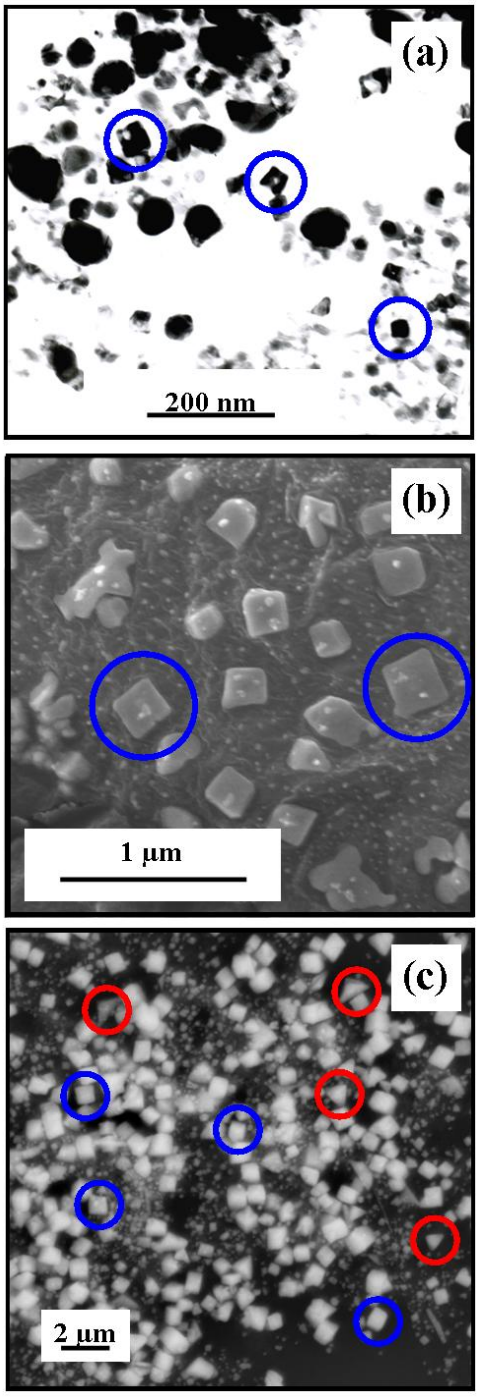

Figure 4. (a) TEM micrograph of typical Ag NPs synthesised using the extract of *Eucalyptus macrocarpa* leaves (s_1), (b) FESEM image of Ag nanocubes and (c) FESEM image of aged Ag particles revealing the presence of cubes and triangular shapes.

Further investigations are needed in order to determine the functional groups present in the *Eucalyptus macrocarpa* leaf extract that are involved in the reducing, capping and stabilizing the Ag NPs. In addition, the antimicrobial properties of the synthesised Ag NPs need to be investigated along with any potential synergistic effects resulting from the leaf extract. Earlier studies by Murata *et al* isolated a novel antibacterial compound (macrocarpal A), while subsequent studies by Yamakoshi *et al* isolated a further six antibacterial compounds (macrocarpal B to G) from *Eucalyptus macrocarpa* leaf extracts [30, 31]. In their studies the structure of the macrocarpal compounds were determined using both XRD and NMR analysis, which revealed that the compounds were composed of phloroglucinol dialdehyde diterpene derivatives. At this stage it is not known if these compounds are involved in the synthesis of the Ag NPs, or whether these compounds could have a potential synergistic effect when used in conjunction with the Ag NPs.

4. Conclusion

In this study, a natural, clean and environmentally friendly plant based agent was used to synthesis Ag NPs. The study for the first time demonstrated the ability of an indigenous Australian plant leaf extract derived from *Eucalyptus macrocarpa* to rapidly synthesis stable Ag nanocubes and other morphologies. The synthesis process was performed at room temperature and the leaf extract performed as both reducing agent and stabilising agent. The Ag NPs synthesised from $AgNO_3$ treated leaf extract were found to have an UV-visible absorption peak at 430 nm, while the mean crystallite size was calculated from XRD data and found to be 38 ± 2 nm. TEM micrographs of the resultant Ag NPs indicate the presence of both spherical and cubic morphologies. The spherical Ag NPs ranged in size from 10 to 100 nm, while the nanometre sized cubes ranged in size from 10 to 50 nm. Subsequent FESEM images of $AgNO_3$/leaf extract mixtures taken after a sufficient aging period, usually several hours, the predominant morphology is cubic and is in the range from 50 nm up to 1 μm.

Acknowledgements

This work was partly supported by the Western Australian Nanochemistry Research Institute (WANRI). The authors would also like to thank Mr Ravi Krishna Brundavanam for his assistance with the XRD measurements and Ms Xuan Le with the FESEM images.

Disclosure

The authors report no conflict of interest in this work.

References

1. R. A. Sperling, P. R. Gil, F. Zhang, M. Zanella and W. J. Parak, Biological applications of gold nanoparticles, Chem. Soc. Rev. 37, 1896-1908 (2008).
2. W. Cai, T. Gao, H. Hong, and J. Sun, Applications of gold nanoparticles in cancer nanotechnology, Nanotechnology, Science and Applications. 1, 17-32 (2008).
3. J. Ramyadevi, K. Jeyassubramanian, A. Marikani, G. Rajakumar and A. A. Rahuman, Synthetic and antimicrobial activity of copper nanoparticles, Mater. Lett. 71, 114-116 (2012).
4. V. K. Sharma, R. A. Yngard and Y. Lin, Silver nanoparticles: Green synthesis and their antimicrobial activities, Advances in Colloid and Interface Science. 145, 83-96 (2009).
5. H. Yan, S. H. Park, G. Finkelstein, J. H. Reif and T. H. La Bean, DNA-templated self-assembly of protein arrays and highly conductive Nanowires, Science. 301, 1882-1884 (2003).
6. K. Keren, R. S. Berman, E. Buchstab, U. Sivan and E. Braun, DNA-templated carbon nanotube field-effect transistor, Science. 302: 1380-1382 (2003).
7. X. Chen and H. J. Schluesener, Nanosilver: A nanoproduct in medical applications, Toxicology letters. 176 (4), 1-12 (2008).
8. R. Brayner, R. Ferrari-Iliou, N. Brivois, S. Djediat, M. Benedetti and F. Fiévet, Toxicological impact studies based on Escherichia coli bacteria in ultrafine ZnO nanoparticles colloidal medium, Nano Letters. 6, 866–870 (2006).
9. A. Simon-Deckers, S. Loo, M. Mayne-L'hermite, N. Herlin-Boime, N. Menguy, C. Reynaud, B. Gouget and M. Carrie, Size composition and shape dependent toxicological impact of metal oxide nano-particles and carbon nano-tubes toward bacteria. Environmental Science Technology. 43, 8423–8429 (2009).
10. J. Ai, E. Biazar, M. Jafarpour, M. Montazeri, A. Majdi, S. Aminifard, M. Zafari, H. R. Akbari and H. G. Rad, Nanotoxicology and nanoparticle safety in biomedical designs. International Journal of Nanomedicine. 6, 1117-1127 (2011).
11. D. Philip, Green synthesis of gold and silver nanoparticles using Hibiscus rosa sinensis, Physica E. 42, 1417-1424 (2010).
12. P. Kumar, P. Singh, K. Kumari, S. Mozumdar and R. Chandra, A green approach for the synthesis of gold nanotriangles using aqueous leaf extract of Callistemon viminalis. Mater. Lett. 65, 595-597 (2011).
13. M. Lengke and G. Southam, Bioaccumulation of gold by sulphate-reducing bacteria cultured in the presence of gold (I)-thiosulfate complex. Acta. 70 (14), 3646-3661 (2006).
14. T. Klaus-Joerger, R. Joerger, E. Olsson and C. Granqvist , Bacteria as workers in the living factory: metal accumulating bacteria and their potential for material science. Trends Biotechnology. 19, 15-20 (2001).
15. A. Ahmad, S. Senapati, M. I. Khan, R. Kumar, R. Ramani, V. Srinivas and M. Sastry, Intracellular synthesis of gold nanoparticles by a novel alkalotolerant actinomycete, Rhodococcus species, Nanotechnology. 14 (7), 824-828 (2003).
16. C. Kuber and S. F. Souza, Extracellular biosynthesis of silver nanoparticles using the fungus *Aspergillus fumigates*. Coll. Surf. B. 47, 160-164 (2006).
17. A. Ahmad, S. Senapati, M. I. Khan, R. Kumar and M. Sastry, Extracellular biosynthesis of monodisperse gold nanoparticles by a novel extremophillic actinomycete, Thermomonospora species. Langmuir. 19 (8), 3550-3553 (2003).
18. K. Simkist and K. M. Wilbur, Mulluscs-epithelial control of matrix and minerals, in Biomineralisation, cell biology and mineral deposition, K. Simkist and K. M. Wilbur, eds. (Academic Press, 1989), p. 231-256.
19. G.V. White, P. Kerscher, R. M. Brown, J. D. Morella, W. McAllister, D. Dean and C. L. Kitchens, Green synthesis of ro-

bust, biocompatible silver nanoparticles using garlic extract, Journal of Nanomaterials. 730746, 1-12 (2012).
20. K. K. Y. Wong, X. L. Liu, Silver nanoparticles: the real ''silver bullet'' in clinical medicine? Med. Chem. Comm. 1, 125–131 (2010).
21. Y. Huang, X. Li, Z. Liao, G. Zhang, Q. Liu, J. Tang, Y. Peng, X. Liu, and Q. Luo, A randomized comparative trial between Acticoat and SD-Ag in the treatment of residual burn wounds including safety analysis, Burns. 33 (2), 161–166 (2007).
22. S. G. Cox, L. Cullingworth and H. Rode, Treatment of paediatricburns with a nanocrystalline silver dressing compared with standard wound care in a burns unit: a cost analysis, South African Medical Journal. 101 (10), 728–731 (2011).
23. M. S. Cohen, J. M. Stern, A. J. Vanni, R. S. Kelley, E. Baumgart, D. Field, J. A. Libertino and I. C. Summerhayes, In vitro analysis of a nanocrystalline silver-coated surgical mesh. Surg. Infect. 8 (3), 397–403 (2007).
24. R. P. Cincotta, J. Wisnewski and R. Engelman, Human population in the biodiversity hotspots. Nature. 404, 990-992 (2000).
25. http://eol.org/pages/635316/overview Encyclopaedia of Life: Eucalyptus Macrocarpa. Last accessed January 21 2013.
26. G. E. J. Poinern, X. T. Le and D. Fawcett, Super-hydrophobic nature of nanostructures on an indigenous Australian eucalyptus plant and its potential application. Nanotechnology, Science and Applications. 4, 113-121 (2011).
27. C. Singh C, V. Sharma, P. K. Naik, V. Khandelwal and H. Singh, A green biogenic approach for synthesis of gold and silver nanoparticles using *Zingiber officinale*, Digest Journal of Nanomaterials and Biostructures. 6 (2), 535-542 (2011).
28. S. A. Masurkar, P. R. Chaudhari, V. B. Shidore and S. P. Kamble, Effect of biologically synthesised silver nanoparticles on *Straphylococcus aureus* biofilm quenching and prevention of biofilm formation, IET Nanobiotechnol. 6 (3), 110-114 (2012).
29. N. Vigneshwaran, N. M. Ashtaputre, P. V. Varadarajan, R. P. Nachane, K. M. Paralikar and A. Balasubramanya, Biological synthesis of silver nanoparticles using the fungus *Aspergillus flavus*. Mater. Lett. 61, 1413-1418 (2007).
30. M. Murata, Y. Yamakoshi, S. Homma, K. Aida, K. Hori and Y. Ohashi, Macrocarpal A, a novel antibacterial compound from *Eucalyptus macrocarpa*, Agric. Biol. Chem. 54 (12), 3221-3226 (1990).
31. Y. Yamakoshi, M. Murata, A. Shimizu and S. Homma, Isolation and characterization of macrocarpals B-G Antibacterial compounds from *Eucalyptus macrocarpa*, Biosci. Biotech. Biochem. 56 (10), 1570-1576 (1992).